Scientific Research Publishing

Atmospheric and Climate Sciences, 2025, 15(1), 248-274
https://www.scirp.org/journal/acs
ISSN Online: 2160-0422
ISSN Print: 2160-0414

Variations in Atmospheric Electromagnetism and Their Impacts on Mortality Rates in the Southern and Northeastern Regions of Brazil

Rose Ane Pereira de Freitas[1*], Julio Renato Quevedo Marques[1], Reynerth Pereira da Costa[2], Júlia Alves Menezes[3], Isabela de Brito Ferreira[4], Rhavena Barbosa dos Santos[5], Ulisses Eugenio Cavalcanti Confalonieri[6]

[1]Department of Meteorology, Federal University of Pelotas (UFPel), Pelotas, Brazil
[2]National Observatory (ON), Ministry of Science, Rio de Janeiro, Brazil
[3]Laboratory of Analysis and Development of Indicators for Sustainability (LADIS), Division of Impacts, Adaptation, and Vulnerability (DIIAV), National Institute for Space Research (INPE), São José dos Campos, Brazil
[4]Department of Parasitology, Institute of Biological Sciences, Federal University of Minas Gerais (UFMG), Belo Horizonte, Brazil
[5]Department of Nursing and Medicine, Federal University of Viçosa (UFV), Viçosa, Brazil
[6]Department of Food Technology, Federal Fluminense University (UFF), and Rene Rachou Institute, Fiocruz, Belo Horizonte, Brazil
Email: *freitas.rose@ufpel.edu.br

How to cite this paper: Freitas, R.A.P., Marques, J.R.Q., Costa, R.P., Menezes, J.A., Ferreira, I.B., Santos, R.B. and Confalonieri, U.E.C. (2025) Variations in Atmospheric Electromagnetism and Their Impacts on Mortality Rates in the Southern and Northeastern Regions of Brazil. *Atmospheric and Climate Sciences*, **15**, 248-274.
https://doi.org/10.4236/acs.2025.151012

Received: November 23, 2024
Accepted: January 21, 2025
Published: January 24, 2025

Abstract

This study examines the relationship between geomagnetic indices and mortality rates from specific diseases in the Northeast (NE) and Southern (S) regions of Brazil from 1996 to 2020. Solar activity data, including the Ap and Sudden Ionospheric Disturbance (SID) indices, were sourced from the World Data Center, while mortality data were obtained from the Mortality Information System (SIM-DATASUS). Acute Myocardial Infarction (AMI) emerged as the leading cause of mortality, with average death rates of 60.4, 56.8, and 58.3 deaths per 100,000 inhabitants in Pernambuco (PE), Rio Grande do Sul (RS), and Paraná (PR), respectively. Temporal analysis revealed a consistent upward trend in AMI mortality across most states, except for Santa Catarina (SC). Seasonal patterns identified through Principal Component Analysis (PCA) demonstrated that geomagnetic and climatic indices influenced mortality differently across regions and seasons. The Ap geomagnetic index was strongly correlated with higher AMI mortality rates during summer, while the SID index showed greater relevance during winter. A dipole phenomenon was observed, with AMI deaths increasing alongside geomagnetic activity in the S region but showing an inverse relationship in the NE region. These findings highlight the significant influence of geomagnetic variations on public health, particularly cardiovascular mortality. The study underscores the need for further research into the biological mechanisms underlying these associations

and recommends the development of early warning systems and targeted preventive measures to mitigate the potential health impacts of geomagnetic disturbances, especially for vulnerable populations.

Keywords

Solar Activity, Cardiovascular Mortality, Geomagnetic Disturbances

1. Introduction

Human exposure to electromagnetic radiation (EMR) has been studied for decades, particularly in relation to non-natural sources [1] [2]. Recently, this field has gained attention due to the advent of 5G technology [3]. However, the potential effects of electromagnetic radiation from natural sources on human health have also been explored in recent decades [4]. Geomagnetic effects are more pronounced at higher magnetic latitudes, with extreme values (both high and low) of geomagnetic activity having adverse effects on health, particularly in sensitive subgroups of the population, with predominant impacts on the cardiovascular system [5]-[7]. Beyond its effects on the cardiovascular system, studies have revealed associations between solar activity peaks and viral epidemics, such as influenza [8]. Specifically, regarding the effects of atmospheric EMR on human health, adverse outcomes have been observed in the cardiovascular system [9]-[11]; infectious diseases [8]; the nervous system [12]; autoimmune diseases [13]; mental health disorders [14]; and mortality from various causes [15] [16], significantly impacting populations at different latitudes.

Growing scientific evidence supports the hypothesis that geomagnetic disturbances can induce biological effects, including non-specific adaptive responses in the human body [16]. Weak variations in the Earth's magnetic field caused by solar and geomagnetic activity may directly influence human physiological parameters. [16] emphasize that global research confirms correlations between "space weather" phenomena, such as solar flares and coronal mass ejections, and fluctuations in the cardiovascular and nervous systems. For example, [9] identified a correlation between increased solar wind intensity and elevated heart rates in Saudi Arabia, suggesting that environmental energetic phenomena may affect psychophysiological processes. Similarly, [17] observed a decrease in heart rate variability (HRV) during geomagnetic storms and an inverse relationship between blood pressure variability and sunspot numbers.

In terms of geographic variation, studies such as the Tbilisi and Piraeus projects [16] have shown that different types of cardiac arrhythmias are correlated with solar and geomagnetic activity. [18] detected an association between geomagnetic disturbances and deaths from cardiovascular diseases in 263 U.S. cities, while [19] identified correlations between solar activity and myocardial infarctions in Lithuania, with stronger correlations among women. Recent findings by [18] suggest that geomagnetic storms and solar proton events may influence ischemic heart

disease mortality, with older men being particularly vulnerable.

Despite compelling evidence of the physiological effects of geomagnetic disturbances, most studies have focused on high and mid-latitudes, leaving a gap in understanding the potential impacts at lower latitudes. [20] highlighted particularities in studies conducted in middle and low geomagnetic latitudes in the Americas, where higher vulnerability among men and a seasonal pattern in infarctions were observed, suggesting that geomagnetic activity and solar cycles influence these risks.

Although promising data exist, the relationship between HRV and geomagnetic activity remains debated. [17] and [21] found conflicting results, while [22] identified significant correlations between HRV and geomagnetic indices. However, after correcting for autocorrelation in time-series data, these correlations were weak, raising concerns that prior studies may have been influenced by data autocorrelation rather than true causal relationships. These findings underscore the need for robust methodologies to interpret these associations accurately.

This study seeks to address these gaps by analyzing the relationship between solar activity variability and mortality from epidemiological events in Brazil's Northeast (NE) and South (S) regions from 1996 to 2020, with a specific focus on Solar Cycles 23 and 24. Statistical and temporal trend analyses were performed to evaluate the impact of solar activity on human health. The influence of geomagnetic and climatic indices on death rates was also investigated, focusing on diseases such as Alzheimer's Disease (AD), Stroke (STK), Multiple Sclerosis (MS), Acute Myocardial Infarction (AMI), Systemic Lupus Erythematosus (SLE), Parkinson's Disease (PD), and Pneumonia (PNM). These findings aim to contribute to a deeper understanding of the complex relationships between environmental factors, solar activity, and public health, providing valuable insights for future research and health policies.

2. Materials and Methods

This study spans the period from 1996 to 2020, corresponding to Solar Cycles 23 and 24, involving the use of monthly, annual, and seasonal averages of geomagnetic activity data and mortality rates associated with specific diseases in the southern and northeastern regions of Brazil. The selection of these regions was based on the significant variation in geomagnetic activity at higher latitudes compared to the Earth's equator. Additionally, extreme values of geomagnetic activity (high or low) have more adverse impacts on health, especially in subgroups of the population considered more sensitive to these adverse effects [7].

2.1. Study Area

This study focuses on the Northeast (NE) and South (S) regions of Brazil. According to the Brazilian Institute of Geography and Statistics (IBGE) [23], the South region covers an area of approximately 564,000 km^2, while the Northeast encompasses 1,554,257 km^2, making it the second most populous region in Brazil (**Figure 1**).

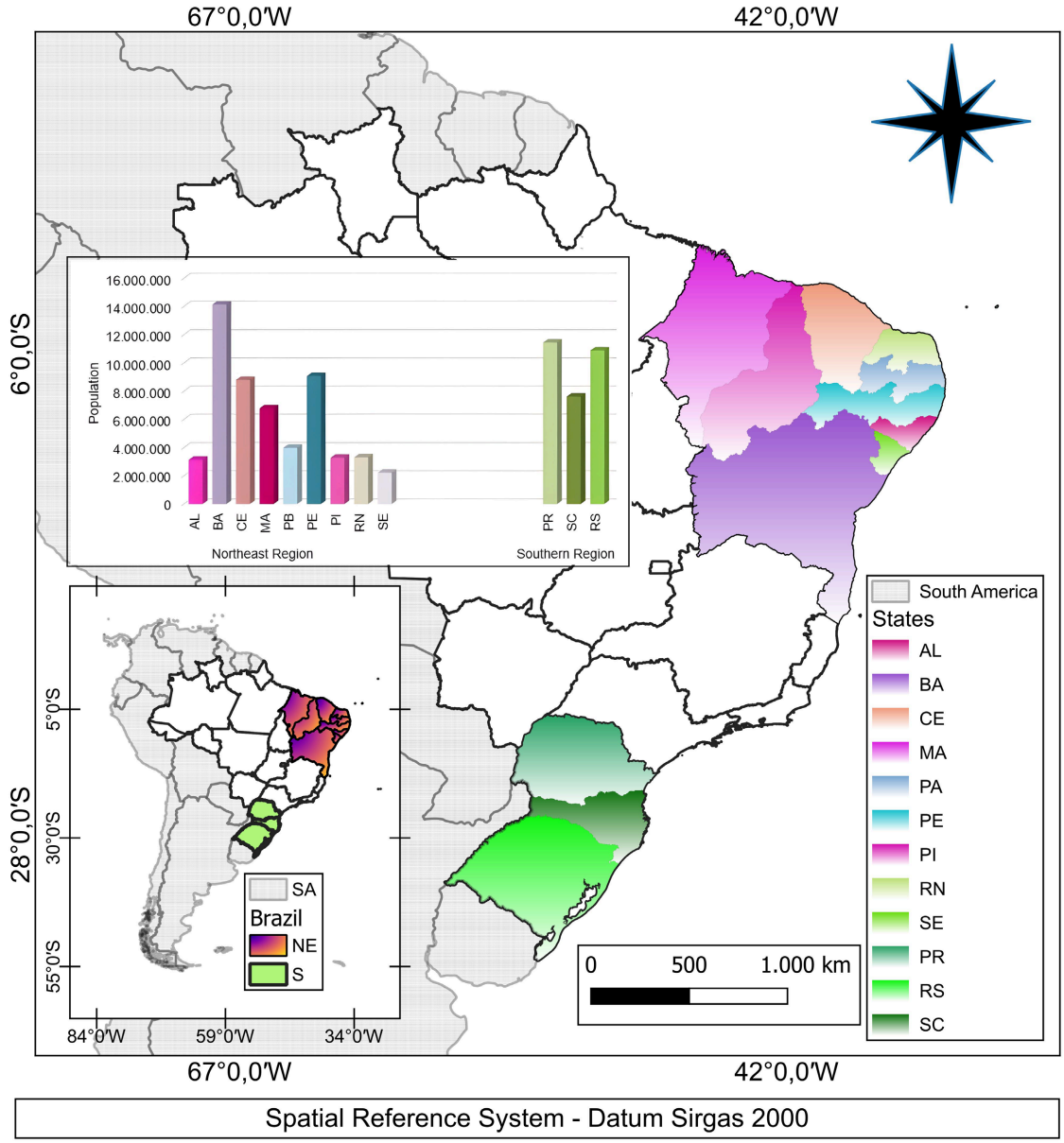

Figure 1. Geographic distribution of the states analyzed in the Northeast (NE) and South (S) regions of Brazil. The main map highlights individual states with color coding: AL (Alagoas), BA (Bahia), CE (Ceará), MA (Maranhão), PB (Paraíba), PE (Pernambuco), PI (Piauí), RN (Rio Grande do Norte), SE (Sergipe) in the Northeast; and PR (Paraná), RS (Rio Grande do Sul), SC (Santa Catarina) in the South. Insets provide additional details: a bar chart comparing the population of states within each region, and a locator map showing the spatial position of Brazil within South America.

2.1.1. The Northeast Region of Brazil

The climate of the Northeast (NE) region is primarily classified as Tropical Savanna (Köppen: Aw), characterized by well-defined wet and dry seasons and an average annual temperature above 18˚C [24]. Precipitation is concentrated in the summer months, while some coastal areas, especially near the Atlantic Ocean, are classified as Tropical Wet (Köppen: Am), with high temperatures and year-round precipitation. Semi-arid conditions (Köppen: BSh) prevail in parts of the interior, particularly in Bahia (BA), where rainfall is scarce and temperatures are high.

The Köppen-Geiger climate classification system, initially developed by Wladimir Köppen and later updated by Rudolf Geiger, provides a standardized framework for understanding regional climates. This system is widely used in epidemiological studies to analyze climatic influences on health outcomes. The updated mapping by [24] further refines these classifications for global applicability.

Disparities in healthcare infrastructure and service quality persist, particularly in rural and semi-arid areas [13] [25]. Efforts to improve public healthcare infrastructure aim to increase access and mitigate these disparities.

2.1.2. The Southern Region of Brazil

The Southern Region of Brazil is characterized by a temperate climate and a diversified economy. Located between latitudes 22˚S and 33˚S and longitudes 48˚W and 57˚W, it comprises three states: Paraná (PR; 11,443,208 inhabitants), Santa Catarina (SC; 7,609,601 inhabitants), and Rio Grande do Sul (RS; 10,880,506 inhabitants), with a combined population of approximately 29,933,315 people [26].

The predominant climate in this region is Humid Subtropical (Köppen: Cfa), featuring four well-defined seasons with hot summers and cold winters. Precipitation is evenly distributed throughout the year. In parts of western Paraná (PR), the climate may be classified as Humid Subtropical Highland (Köppen: Cfb), where temperatures are milder due to higher altitudes [24].

According to data from the Brazilian Institute of Geography and Statistics [26], the Southern Region has a lower population density compared to other regions in Brazil. Major cities include Curitiba (PR), Florianópolis (SC), and Porto Alegre (RS). The region boasts a higher per capita income compared to the national average, supported by a diversified economy encompassing agriculture, industry, and services, contributing to a relatively high quality of life.

Healthcare services in the Southern Region are more accessible and exhibit favorable indicators compared to regions such as the Northeast (NE). The region has one of the highest concentrations of physicians per thousand inhabitants, with a significant distribution in inland areas. For example, in SC, 70.8% of doctors practice in inland areas, while in Sergipe (SE), a state in the NE, 91.8% of doctors are concentrated in the capital, Aracaju [13].

2.2. Mortality Data

The mortality data analyzed in this study were obtained from the Mortality Information System (SIM), provided by the Department of Informatics of the Unified Health System (DATASUS). The 10th revision of the International Classification of Diseases, Brazilian version (ICD-10 BR), was used to classify epidemiological outcomes, including neurodegenerative diseases, infectious diseases, autoimmune diseases, and all-cause mortality.

The study focused on the NE and S regions of Brazil (**Figure 1**). Data on the estimated resident population in each state were sourced from IBGE [26]. The mortality data were filtered by state, month, year of death, and cause of death as defined by ICD-10, covering the period from 1996 to 2020.

The mortality rate (MR) was calculated using the following formula:

$$MR = \frac{\text{Absolut number of deaths per cause per month/year}}{\text{Total population of the state in the same period}} \times 100000 \quad (1)$$

2.3. Solar and Geomagnetic Activity Data

The solar activity data used in this study include the Sunspot Number (SN) and the F10.7 index, both of which are solar indices. Additionally, Sudden Ionospheric Disturbances (SIDs) were analyzed, representing ionospheric disturbances caused by solar flares. The geophysical data used are limited to the Kp and Ap indices, which measure geomagnetic activity. It is essential to classify these indices accurately according to their nature, as they are interrelated but serve distinct roles.

The Sunspot Number (SN) is a direct measure of solar activity, based on the number of visible sunspots on the Sun's surface. This index is calculated by averaging daily sunspot counts to derive annual values. The data are provided by the WDC-SILSO (World Data Center - Sunspot Index and Long-term Solar Observations) from the Solar Influences Data Analysis Center (SIDC) at the Royal Observatory of Belgium. In this study, daily sunspot data were used to capture finer temporal variations that might be overlooked in annual averages, enabling a more detailed investigation of potential correlations between solar activity and health outcomes [27].

The F10.7 index, also a direct measure of solar activity, represents the solar radio flux at a wavelength of 10.7 cm. This index is widely used in both short- and long-term analyses of solar variability, as it reliably reflects changes in the Sun's magnetic activity. It is critical for understanding variations in solar radiation and their potential impacts on Earth's atmospheric systems [28].

The Sudden Ionospheric Disturbances (SIDs) index reflects disruptions in Earth's ionosphere caused by solar flares. These disturbances are detected through ionospheric monitoring networks that analyze variations in radio signals, often transmitted by satellite navigation systems. SIDs provide valuable insights into how solar events influence the ionosphere [29] [30].

For geomagnetic activity, this study uses the Kp and Ap indices. The Kp index is a normalized global measure of geomagnetic activity, with values ranging from 0 (quiet conditions) to 9 (extreme disturbances). The Ap index, derived from the Kp index, converts these values into a linear scale (0 - 400), offering a more detailed representation of geomagnetic activity intensity. These indices are widely employed to monitor geomagnetic storms and analyze variations in Earth's magnetic field [31] [32].

This study carefully differentiates the indices: SN and F10.7 as solar indices, SIDs as an ionospheric index, and Kp and Ap as geomagnetic indices. This classification ensures their interrelations and distinct contributions are accurately represented throughout the manuscript.

2.4. Statistical Analyses

This study applied various statistical methods to investigate the spatial and

temporal variations in mortality data. Boxplots were used to visually summarize the distribution of the data, displaying the median, interquartile range (IQR), and potential outliers. This method provides an effective way to detect variability and identify outliers within the dataset [33].

Pearson's correlation coefficient was calculated to assess the strength and direction of the linear relationship between two continuous variables. The coefficient ranges from −1 to 1, where values near −1 indicate a strong negative correlation, 0 indicates no correlation, and values near 1 indicate a strong positive correlation [34].

Least squares linear regression was employed to analyze temporal trends by modeling the relationship between a dependent variable and one or more independent variables. This method fits a line that minimizes the sum of squared residuals, enabling the detection of trends in mortality data over time [35].

Student's t-test was conducted to compare the means of two groups, determining whether they were statistically different. This test assumes the data follows a normal distribution and is commonly used to evaluate differences between group means [36].

Significance levels for correlations were evaluated to determine whether observed relationships between variables were statistically significant. The p-value was used to assess the likelihood that the observed correlation occurred by chance, with a significance threshold commonly set at 0.05 [31].

Principal Component Analysis (PCA) was applied to identify spatial and temporal oscillation patterns in mortality data. PCA reduces the dimensionality of the dataset while preserving variability, facilitating the assessment of relationships among variables and uncovering patterns [37].

Trend removal was also applied to temporal data when necessary, ensuring that analyses focused on seasonal patterns and the impacts of geomagnetic activity and climatic factors. This preprocessing step enhanced the clarity of the results by isolating relevant variations in the data.

3. Results and Discussion

3.1. Geophysical Indices

The analysis of solar activity from 1996 to 2020 revealed significant variability in sunspot numbers (SN), capturing distinct phases of heightened and reduced activity. **Figure 2**, using boxplots, illustrates this variability, highlighting two solar cycles: Solar Cycle 23 (1996-2008) and Solar Cycle 24 (2008-2020). Solar Cycle 23 was characterized by higher activity, with an average sunspot count of 45.8 and peaks reaching approximately 175 sunspots during periods of maximum activity. In contrast, Solar Cycle 24 exhibited lower activity levels, reflecting a general decline in solar intensity [27].

The peaks observed during Solar Cycle 23 indicate periods of elevated solar radiation and geomagnetic disturbances, aligning with intensified space weather effects. Conversely, the lower quartiles correspond to solar minimum phases,

representing periods of reduced solar activity. This cyclical variability is consistent with well-established solar behavior, which directly impacts Earth's ionosphere and geomagnetic field conditions [32].

The quartile plot in **Figure 2** visually conveys these fluctuations, emphasizing the solar maximum and minimum phases across the study period. The substantial range observed in the quartiles reflects the extremes of solar activity and highlights the necessity of examining their correlations with geomagnetic disturbances and mortality data. These findings underscore the relevance of understanding how solar cycles influence geophysical and biological systems, providing a foundation for the subsequent analysis of health impacts [29].

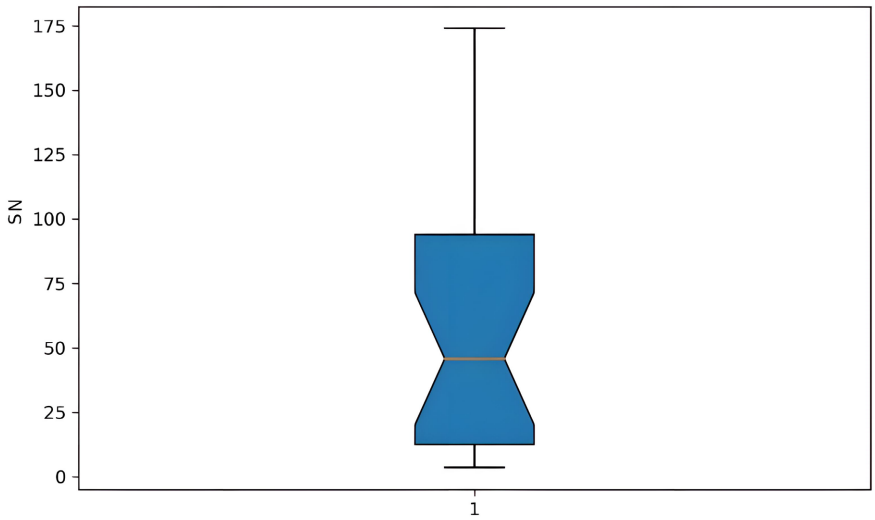

Figure 2. Box plot of the Sunspot Number (SN) distribution for the study period (1996-2020). The plot shows the interquartile range, median, and variability in solar activity, with the y-axis representing the Sunspot Number (SN). This representation highlights the spread of the SN values over the analyzed period.

The indices analyzed in this study—Sunspot Number (SN), Ap Index, Kp Index, and F10.7 Index—highlight variations in solar and geomagnetic activity from 1996 to 2020 (**Figure 3**). Consistent with previous studies, such as those by [27] and [38], significant fluctuations in solar activity were observed across Solar Cycles 23 (1996-2008) and 24 (2008-2020). These variations are particularly evident in the SN, a primary indicator of solar magnetic activity and solar cycle phases, as shown in **Figure 3(a)**.

Solar Cycle 23, considered the longest in the space age [39], was characterized by a moderate activity peak, with the SN reaching values above 200 sunspots per month around the early 2000s. As the cycle progressed, a gradual decline in activity was observed, interspersed with temporary increases in sunspot counts, though they did not match the peak levels. In contrast, Solar Cycle 24, one of the weakest solar cycles in recent history, began with a significant delay in solar activity [32].

According to [32], this delay may signal changes in solar variability, similar to those observed during Solar Cycle 14 (1902-1913). Geomagnetic storm activity

also differed between the cycles, with Solar Cycle 23 recording 22 events of magnitude Kp = 8 (G5), compared to only 7 such events in Solar Cycle 24 [33]. These findings suggest a notable decline in both solar and geomagnetic activity during Solar Cycle 24, potentially reflecting broader trends in solar behavior.

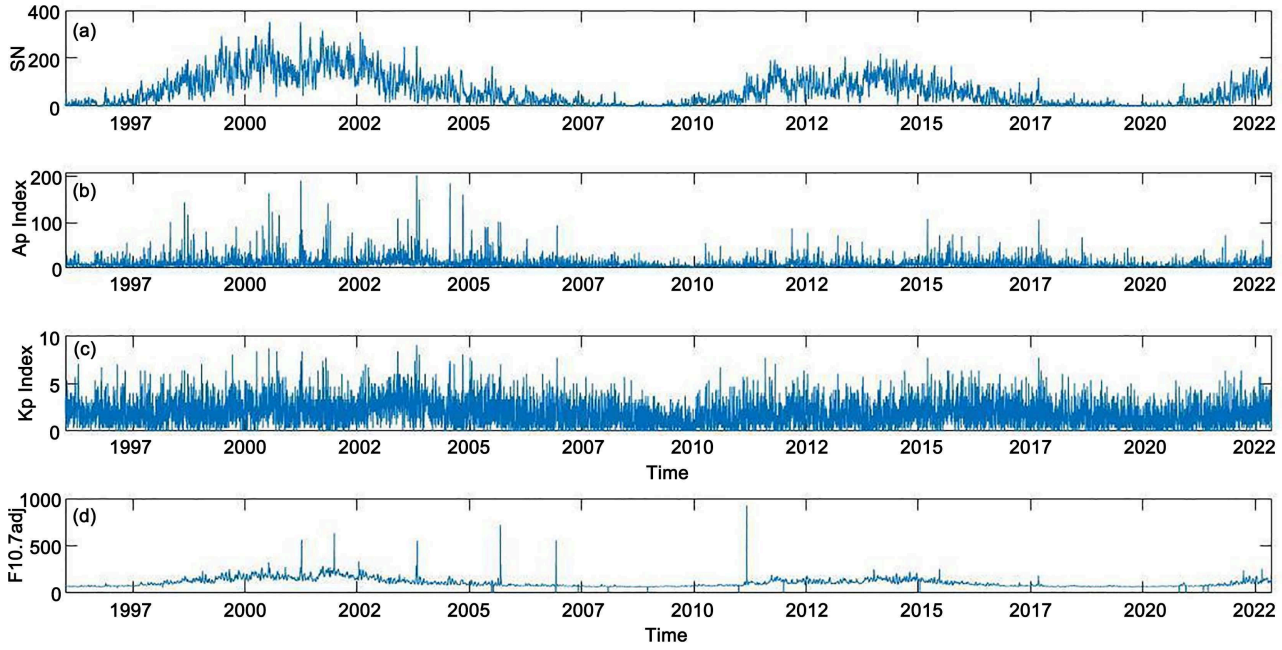

Figure 3. Solar and geomagnetic activity variation during the period 1996-2020 for Solar Cycles 23 and 24. (a) Sunspot Number (SN), representing solar magnetic activity; (b) Ap index, a measure of geomagnetic activity intensity; (c) Kp index, a global measure of geomagnetic activity; and (d) F10.7 index, representing solar radio flux at a wavelength of 10.7 cm. Abbreviations: SN (Sunspot Number), Ap (Ap index), Kp (Kp index), F10.7 (solar radio flux index).

The significant reduction in geomagnetic activity between Solar Cycle 23 and Solar Cycle 24 has been attributed to the smaller size and mid-latitude positioning of coronal holes during this period, as emphasized by [25]. This condition resulted in weaker solar wind speeds and reduced magnetic field fluctuations.

During Solar Cycle 24, the Sunspot Number (SN) remained historically low in the early years, reaching its minimum during 2008-2009. Notably, the cycle's maximum sunspot count was approximately 100 sunspots per month, a marked reduction compared to Solar Cycle 23. These variations are critical for understanding solar activity patterns and their implications for space weather, human health, and technical systems. Despite advances in solar research, accurately predicting solar magnetic activity remains challenging, as noted by [28].

The SN remains a key metric for monitoring solar activity, complemented by other indices such as X-ray flux, the F10.7 index, and magnetic field parameters, providing a comprehensive analysis of solar variability.

[40] identified four distinct phases in Solar Cycle 24: the minimum phase (2008-2009), the ascending phase (2010-2011), the maximum phase (2012-2014), and the descending phase (2015-2018). These phases align with observed correlations between solar activity and death rates in the Northeast (NE) and South (S) regions

of Brazil.

In **Figure 3(b)**, the Ap index reflects considerable variation in geomagnetic activity from 1996 to 2020. During Solar Cycle 23 (1996-2008), the Ap index showed moderate activity with occasional geomagnetic storms but did not reach extreme levels. By contrast, Solar Cycle 24 (2008-2020) exhibited a decreasing trend in the Ap index, which reached its lowest recorded levels. These results are consistent with [29], who noted that geomagnetic activity was influenced by both solar changes and the Earth's position relative to coronal holes.

In **Figure 3(c)**, the Kp index demonstrates the variability in geomagnetic activity. During Solar Cycle 23, the peak occurred around mid-2002, with several significant geomagnetic storms (Kp = 8, classified as G5). These events affected satellite navigation systems, radio communications, and power grids in some regions. Solar Cycle 24, despite weaker solar activity overall, still experienced moderate geomagnetic events, with temporary increases in the Kp index. [41] attributed these fluctuations to interactions between the ionosphere, magnetosphere, and planetary magnetic fields.

In **Figure 3(d)**, the F10.7 index highlights the solar radio flux at 10.7 cm, which exhibited relatively low levels during the early Solar Cycle 23 but peaked twice—first in 2000 and then in 2002, with the latter being stronger. These peaks correspond to periods of intense solar radio emissions and heightened sunspot numbers. As Solar Cycle 23 transitioned into Solar Cycle 24, the F10.7 index gradually decreased, reflecting the overall decline in solar activity.

The F10.7 index, a direct measure of solar activity, correlates with sunspot numbers and serves as a key proxy for tracking fluctuations in solar activity. Sunspots, dark regions of intense magnetic fields on the Sun's surface, directly influence this index, providing insights into broader patterns of solar variability [8] [30].

3.2. Variability of the Mortality Rates

The analysis of mortality data facilitates the identification of temporal trends, differences among demographic and geographic groups, and the investigation of risk factors associated with deaths. Boxplots play a critical role in this context by summarizing statistical measures, identifying outliers, and enabling the comparison of distributions across groups. In **Figure 4**, the boxplot graph illustrates the variability in death rates for each state within the Northeast (NE) and South (S) regions, highlighting specific diseases under study.

The highest death rates in both regions are associated with Stroke (STK), Pneumonia (PNM), and Acute Myocardial Infarction (AMI). Notably, Multiple Sclerosis (MS) exhibits the highest number of outliers, indicating extreme death events that deviate from normal patterns. In contrast, Systemic Lupus Erythematosus (SLE) has the lowest death rate among the diseases analyzed.

Comparing the variability in death rates between the NE and S regions, as shown in **Figure 5**, AMI consistently exhibits the highest average mortality rates in both regions. In the NE, AMI is followed by PNM and STK, whereas in the S region, STK and PNM follow AMI in terms of average death rates. These findings

underscore regional differences and highlight AMI as a leading cause of mortality in both areas example citations, but you can update or modify them based on your reference list. Let me know if you'd like to adjust or expand anything further.

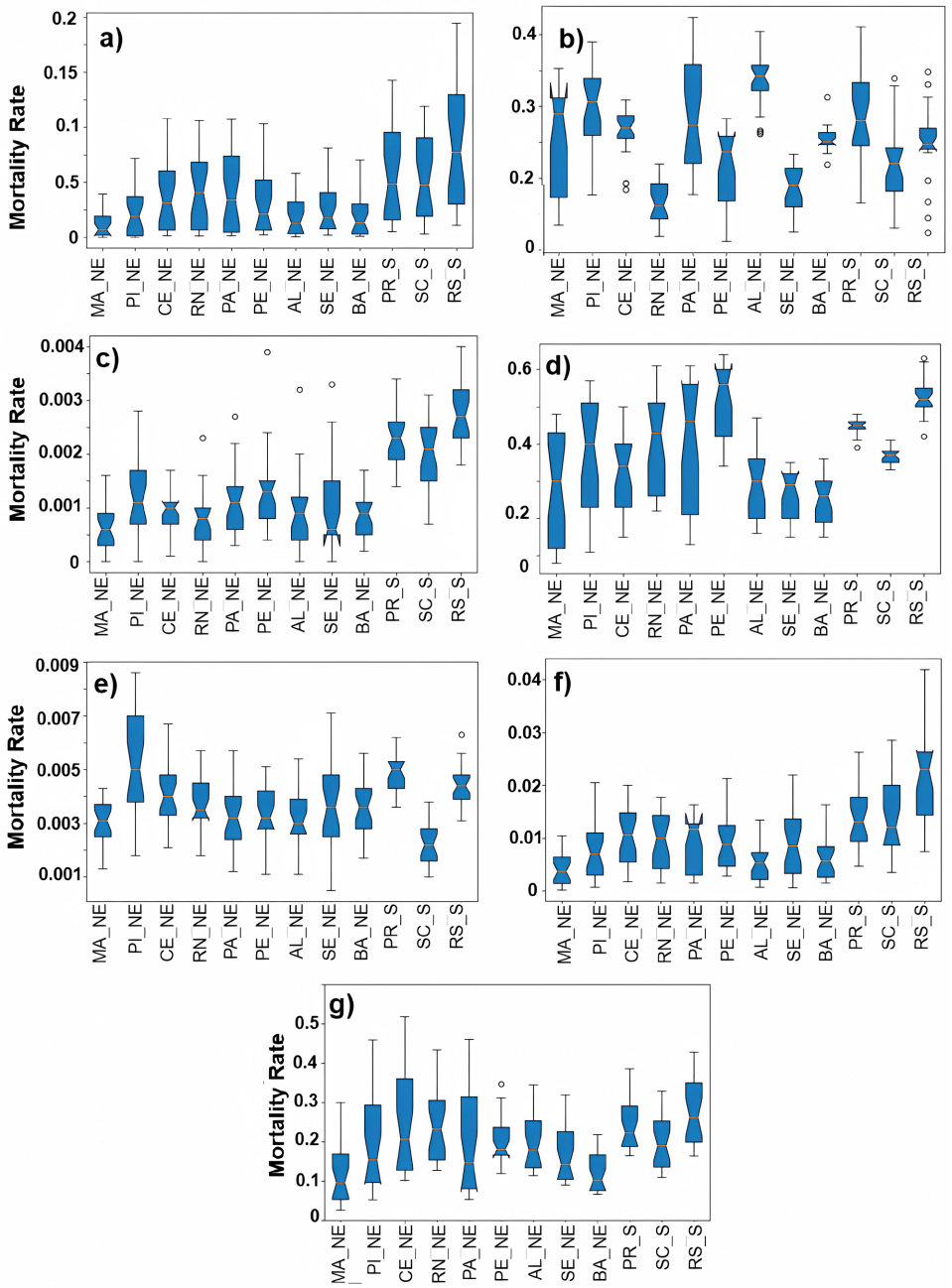

Figure 4. Annual variability of death rates in Brazilian regions from 1996 to 2020 for (a) Alzheimer's Disease (AD), (b) Stroke (STK), (c) Multiple Sclerosis (MS), (d) Acute Myocardial Infarction (AMI), (e) Systemic Lupus Erythematosus (SLE), (f) Parkinson's Disease (PD), and (g) Pneumonia (PNM). The suffixes "NE" and "S" refer to the Northeast and Southern regions, respectively. Each boxplot represents the distribution of mortality rates, where the central line indicates the median, the box spans the interquartile range (IQR) from the 25th percentile (Q1) to the 75th percentile (Q3), and the whiskers extend to 1.5 times the IQR from the box edges. Data points beyond these whiskers are considered outliers and are represented as individual markers.

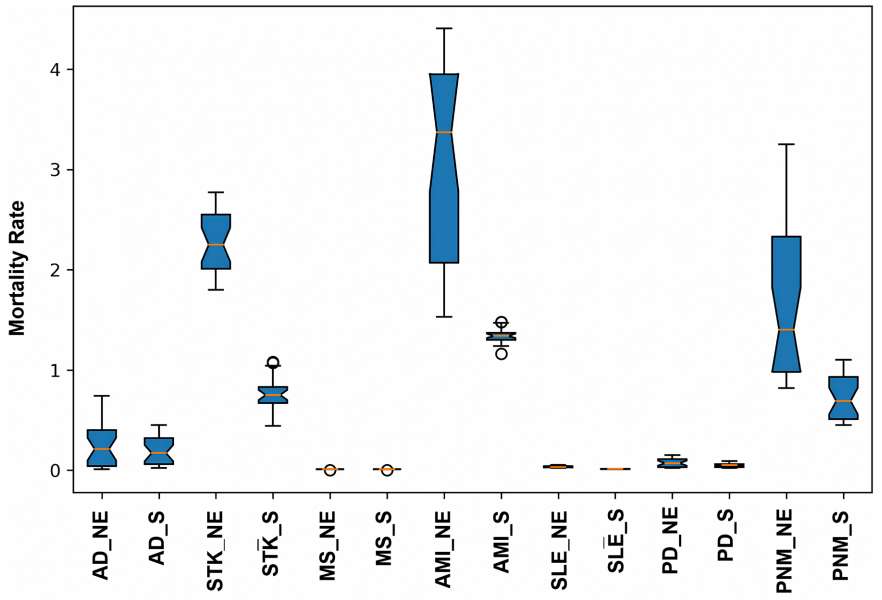

Figure 5. Boxplot illustrating the variability of mortality rates in the Northeast (NE) and Southern (S) regions of Brazil from 1996 to 2020 for the following causes of death: Alzheimer's Disease (AD), Stroke (STK), Multiple Sclerosis (MS), Acute Myocardial Infarction (AMI), Systemic Lupus Erythematosus (SLE), Parkinson's Disease (PD), and Pneumonia (PNM). The x-axis represents the years, while the y-axis displays mortality rates per 100,000 inhabitants. Each boxplot represents the median, interquartile range (IQR), and potential outliers for each disease across the study period.

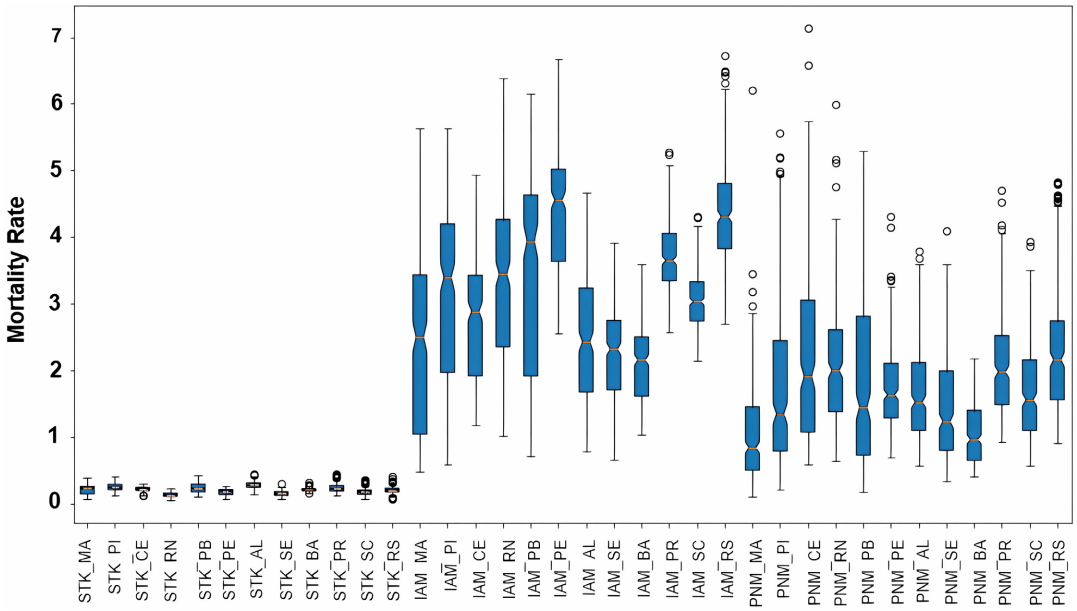

Figure 6. Boxplot illustrating the variability of mortality rates in the Northeast (NE: AL, BA, CE, MA, PB, PE, PI, RN, SE) and Southern (S: PR, RS, SC) regions of Brazil from 1996 to 2020 for the following causes of death: Stroke (STK), Acute Myocardial Infarction (AMI), and Pneumonia (PNM). The suffixes "NE" and "S" indicate the respective regions. Each boxplot represents the distribution of mortality rates, with the central line indicating the median, the box spanning the interquartile range (IQR) from the 25th percentile (Q1) to the 75th percentile (Q3), and whiskers extending to 1.5 times the IQR. Points beyond the whiskers are considered outliers and are displayed as individual markers.

Among the diseases analyzed in this study, the three most representative in both the Northeast (NE) and Southern (S) regions were Stroke (STK), Acute Myocardial Infarction (AMI), and Pneumonia (PNM). To enhance comparability, the original variability of death rates was transformed into standardized anomalies. This method, depicted in Figure 6, standardizes fluctuations based on the mean and standard deviation, allowing for a more precise comparison across regions and diseases.

As shown in Figure 6, the highest mean anomalies for deaths were observed for AMI in both regions, with emphasis on Pernambuco (PE), Rio Grande do Sul (RS), Paraíba (PB), and Paraná (PR). Maximum anomaly values were predominantly concentrated in the NE, particularly in PB, Rio Grande do Norte (RN), and PE. For PNM, the highest mean anomalies were identified in RS, PR, RN, and Ceará (CE), with CE presenting the highest number of deaths and outliers. In contrast, STK-related deaths were the least representative in this analysis.

Given the prominence of AMI-related deaths, a focused analysis was conducted for this event due to its relevance in cardiovascular disease contexts. Figure 7 highlights the highest AMI death rate averages in PE, RS, and PB, indicating a significant concentration of these events in these states. Conversely, the lowest values were observed in Maranhão (MA) and Piauí (PI), revealing notable disparities in AMI mortality between the S and NE regions of Brazil.

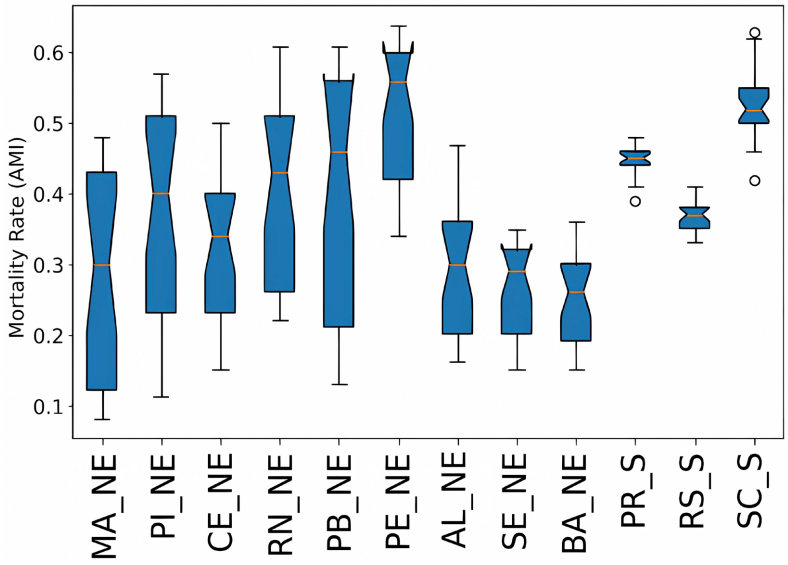

Figure 7. Boxplot illustrating the variability of Acute Myocardial Infarction (AMI) mortality rates across states in the Northeast (NE: AL, BA, CE, MA, PB, PE, PI, RN, SE) and Southern (S: PR, RS, SC) regions of Brazil. The x-axis represents the states, while the y-axis shows mortality rates per 100,000 inhabitants from 1996 to 2020. Each boxplot represents the median, interquartile range (IQR) from the 25th percentile (Q1) to the 75th percentile (Q3), and potential outliers beyond 1.5 times the IQR.

An additional noteworthy aspect is the presence of outliers in AMI death rates

in the S region, as shown in Figure 7. These outlier values warrant further investigation to uncover potential risk factors or demographic characteristics contributing to the variability in AMI-related mortality. Such findings could provide valuable insights for targeted public health interventions.

Temporal trends in AMI death rates were calculated with a statistical significance level of 1%, except in Santa Catarina (SC), where the trend was not statistically significant. To identify and characterize these trends, a least squares fitting approach was applied, plotting death rates against time (in months).

When interpreting the annual variations presented in Figure 4, Figure 6, and Figure 7, it is important to note that while error bars indicate variability, these differences are not always statistically significant. The error bars represent interquartile ranges (IQR), reflecting the data spread. Overlapping error bars across years and states suggest that observed variations may fall within the margin of error. Although the figures visually highlight variability, additional statistical tests, such as ANOVA, were performed to assess the significance of these differences. While detailed results of these tests are not shown here, they indicated that yearly variations generally fell within the expected range of variability and were not statistically significant. As this article focuses on broader spatial and temporal patterns, these calculations were excluded but are available for further discussion if necessary.

Trend analysis and subsequent trend removal were conducted for all states analyzed. In Figure 8, data for two states, Paraná (PR) and Rio Grande do Norte (RN), are presented through scatter plots. These plots display the raw data for AMI deaths and their respective trends over the study period (Table 1). Additionally, the data are shown after trend removal, emphasizing the importance of seasonality, which is evident in the adjusted data.

In the state of Paraná (PR) (Figure 8(a)), the trend analysis reveals a minimal positive slope, described by the equation $y = 0.0036x + 3.68$, with an R^2 value of 0.03. This indicates that the trend minimally explains the variability in AMI deaths over time, suggesting a relatively stable pattern. After removing this trend (Figure 8(b)), the residuals fluctuate around a zero baseline, confirming that the AMI death index has remained fairly constant over the years, with no significant underlying trend. The trend removal emphasizes the random variability in the data, indicating that further modeling is unnecessary.

Table 1. Linear regression equations and corresponding R^2 values for the AMI death index trends in the states of Paraná (PR) and Rio Grande do Norte (RN) over the study period. The equations describe the relationship between time (years) and the AMI death index, while the R^2 values indicate the proportion of variability in the data explained by the linear model for each state.

State	Fitting Equation	R^2 Value
Paraná	$y = 0.0036x + 3.68$	0.03
Rio Grande do Norte	$y = 0.0407x - 76.49$	0.67

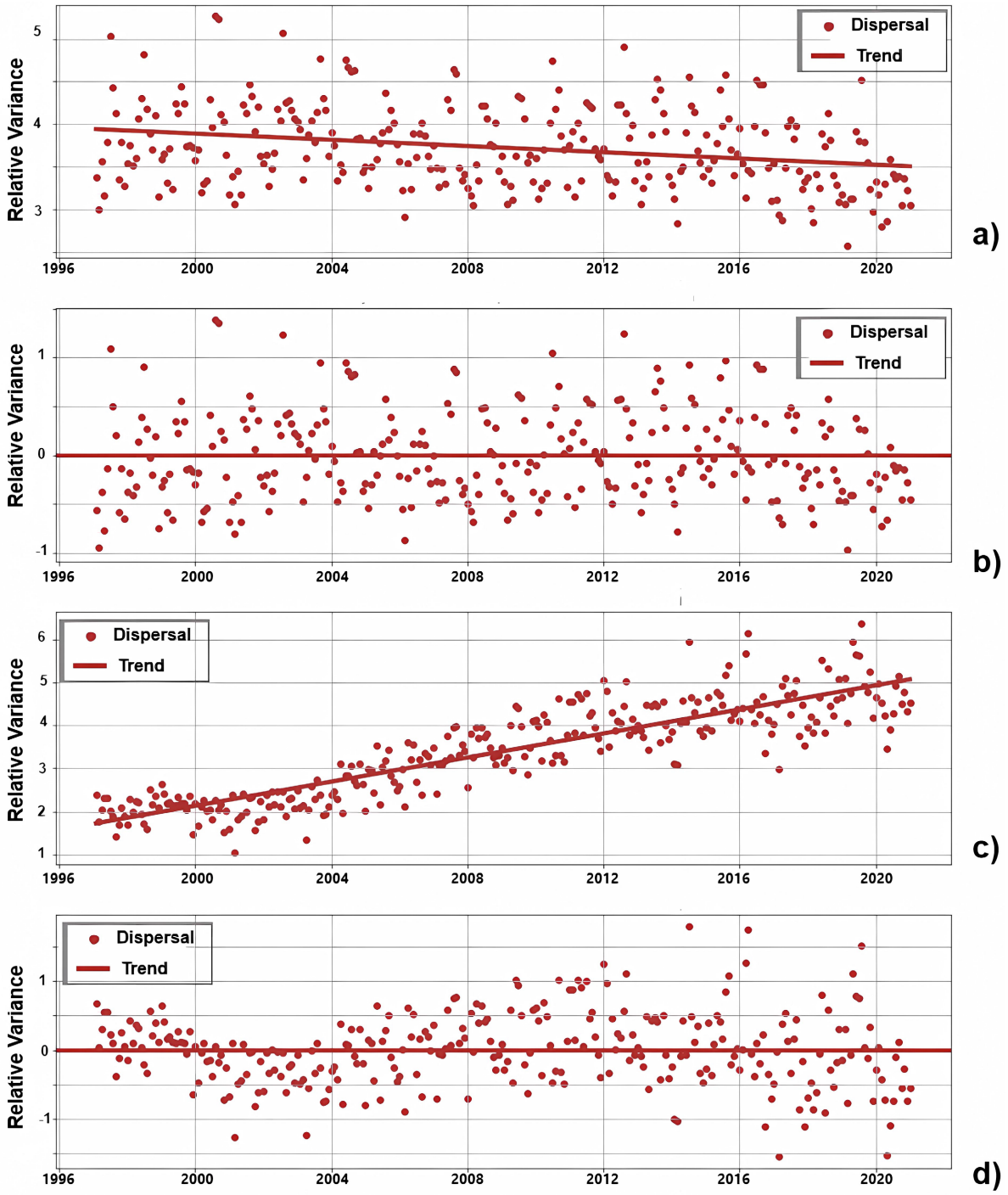

Figure 8. Scatter plots of Acute Myocardial Infarction (AMI) death data for Paraná (PR) and Rio Grande do Norte (RN): (a) Trend analysis for PR, showing the variability of AMI deaths over time, with years on the x-axis and relative variance on the y-axis. (b) Trend removal for PR, displaying the residuals of the AMI death index after subtracting the trend, with years on the x-axis and relative variance on the y-axis. (c) Trend analysis for RN, with years on the x-axis and relative variance on the y-axis. (d) Trend removal for RN, showing the residuals after trend subtraction, with years on the x-axis and relative variance on the y-axis. Axis titles have been enlarged for clarity.

Conversely, in Rio Grande do Norte (RN) (Figure 8(c)), the trend analysis reveals a significant upward slope, described by the equation $y = 0.0407x - 76.49$,

with an R^2 value of 0.67. This indicates that the trend accounts for a substantial portion of the variability in AMI deaths. After removing this trend (**Figure 8(d)**), the residual plot shows data fluctuating around the zero line, confirming that the linear trend effectively captures the increasing pattern in AMI deaths, with no additional trends remaining after adjustment.

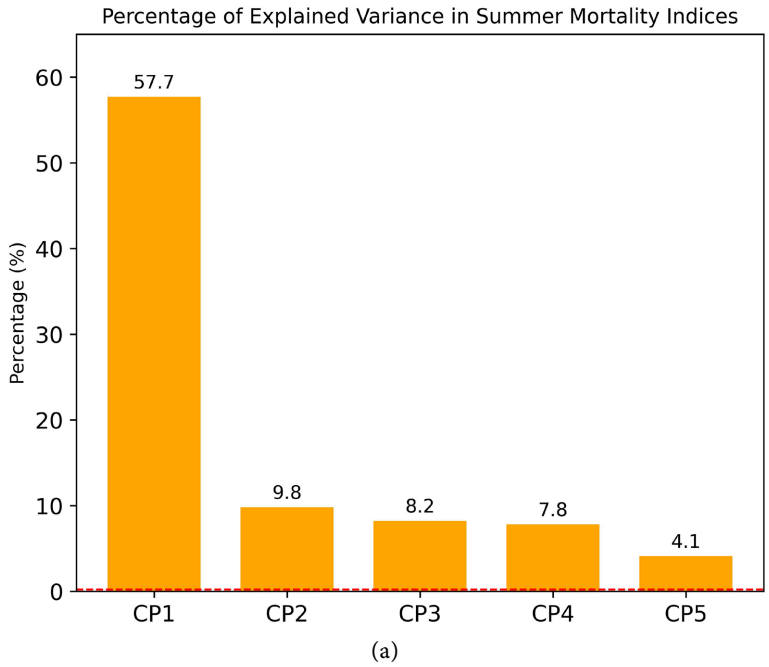

(a)

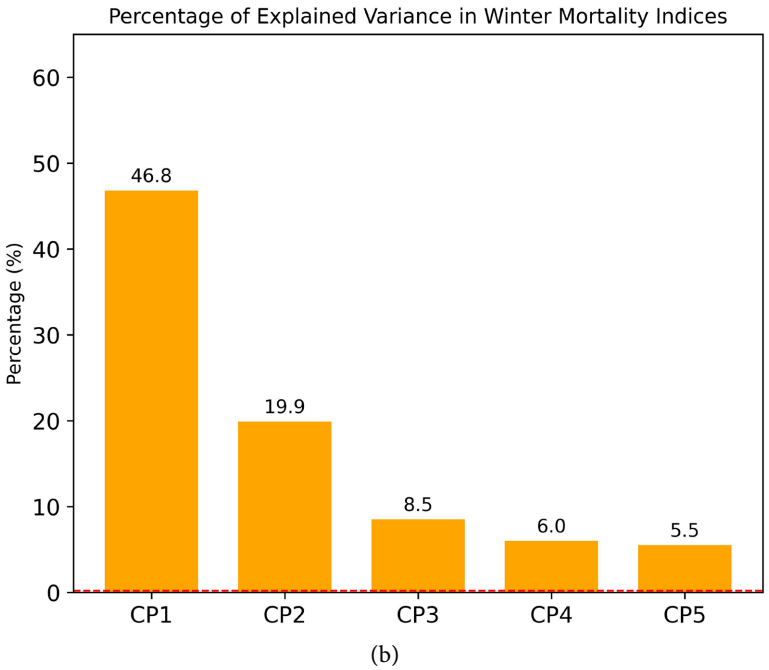

(b)

Figure 9. Percentage of variance explained for AMI death indices in (a) Summer (January-February-March, JFM) and (b) Winter (June-July-August, JJA). The x-axis represents the principal components (PCs), and the y-axis shows the percentage of variance explained by each component for mortality rates during the respective seasons.

Seasonality becomes evident in these figures, highlighting systematic variations in AMI deaths across different months of the year. These seasonal fluctuations are crucial for understanding underlying dynamics and formulating intervention strategies. Specific analyses focusing on months typically associated with summer (January-February-March, JFM) and winter (June-July-August, JJA) in the Southern Hemisphere are essential to fully explore the relationships between solar activity, climatic factors, and the occurrence of AMI deaths.

Principal Component Analysis (PCA) (**Figure 9**), performed on the standardized matrix of AMI data with trends removed, shows that the first principal component explains over 57% of the variance in summer, while in winter, this component accounts for approximately 47%. The second principal component explains about 10% of the variance in summer and 20% in winter. Notably, component decomposition was conducted separately for summer and winter to capture the distinct seasonal patterns.

To identify the state that best represents the combined primary oscillation pattern of AMI in Brazil, correlations were calculated between the scores of the first combined principal component and the individual indices (**Figure 10(a)**). This analysis revealed that Sergipe (SE) and Bahia (BA) are the most representative states in explaining variations during the summer months. For the winter months, Paraná (PR) and Rio Grande do Norte (RN) emerged as more relevant. Notably, the correlation coefficients between these highlighted states are inverse between the seasons, creating a dipole pattern between the locations.

Based on the correlogram presented for winter (**Figure 10(b)**), the results highlight that the AMI mortality index shows a strong negative correlation with the state of Rio Grande do Norte (RN), with a coefficient of −0.82. This pattern reflects the relevance of RN in capturing variations associated with winter seasonal conditions. Conversely, Paraná (PR) exhibited a significant positive correlation (0.53), indicating an inverse relationship between the two regions in terms of AMI mortality variations during winter. These findings reinforce the existence of a dipolar pattern between these locations, suggesting that climatic and geomagnetic factors influencing mortality indices operate differently across these regions during the cold season. These results underscore the importance of detailed spatial analysis to understand the interactions between environmental variables and public health in different regional and seasonal contexts in Brazil.

Although numerous studies in recent decades have explored the effects of artificial electromagnetic fields (EMFs) on human health, particularly in relation to childhood leukemia, fewer studies have investigated the potential effects of exposure to natural radiation from the magnetosphere. Regarding possible biophysical interaction mechanisms explaining the effects of non-ionizing EMFs on human physiology, proposed hypotheses include genotoxicity, suppression of melatonin secretion, increased tissue free radical concentrations, and altered calcium ion homeostasis. Furthermore, it has been suggested that Schumann Resonance signals could act as a global signal absorbed by the human body, linking geomagnetic activity to human health.

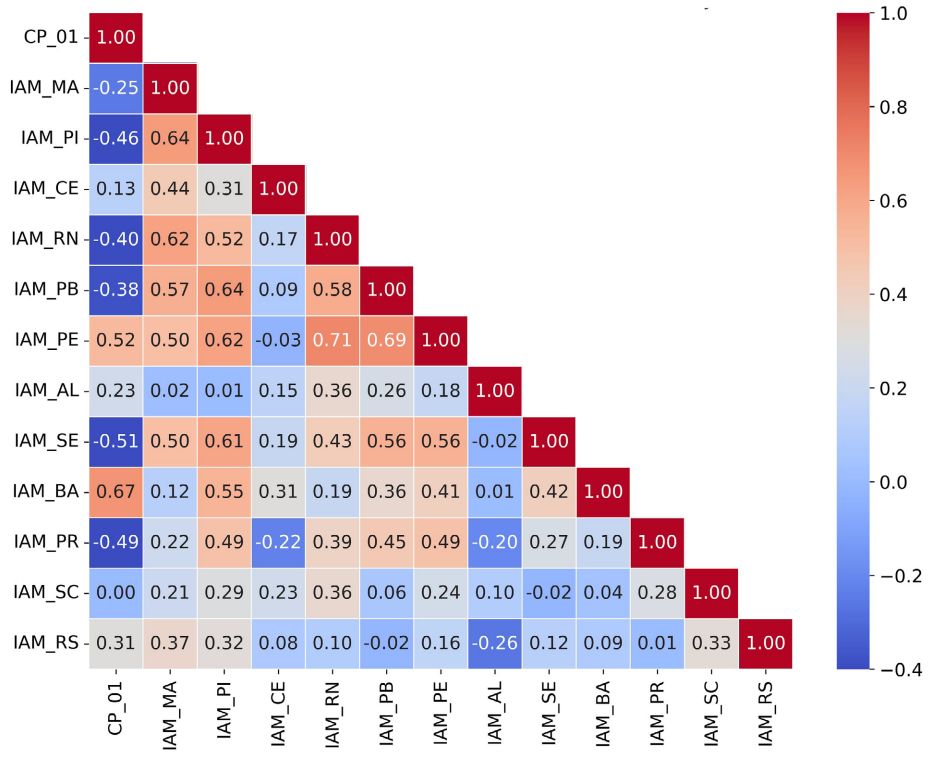

(a)

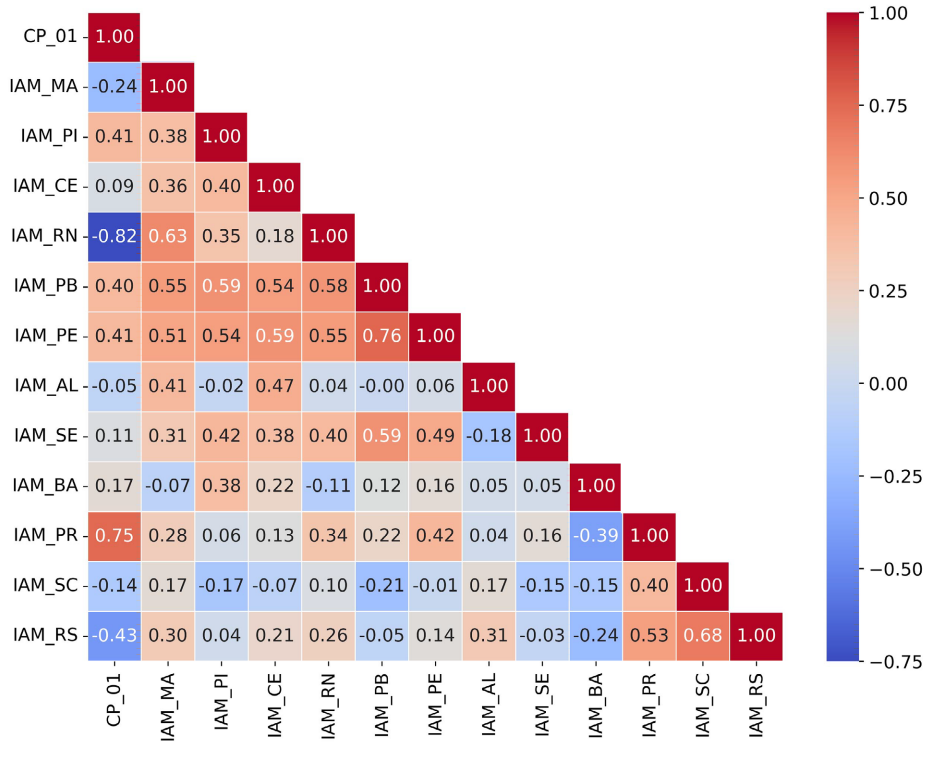

(b)

Figure 10. Correlation between the first principal component scores and AMI death indices, summer and winter.

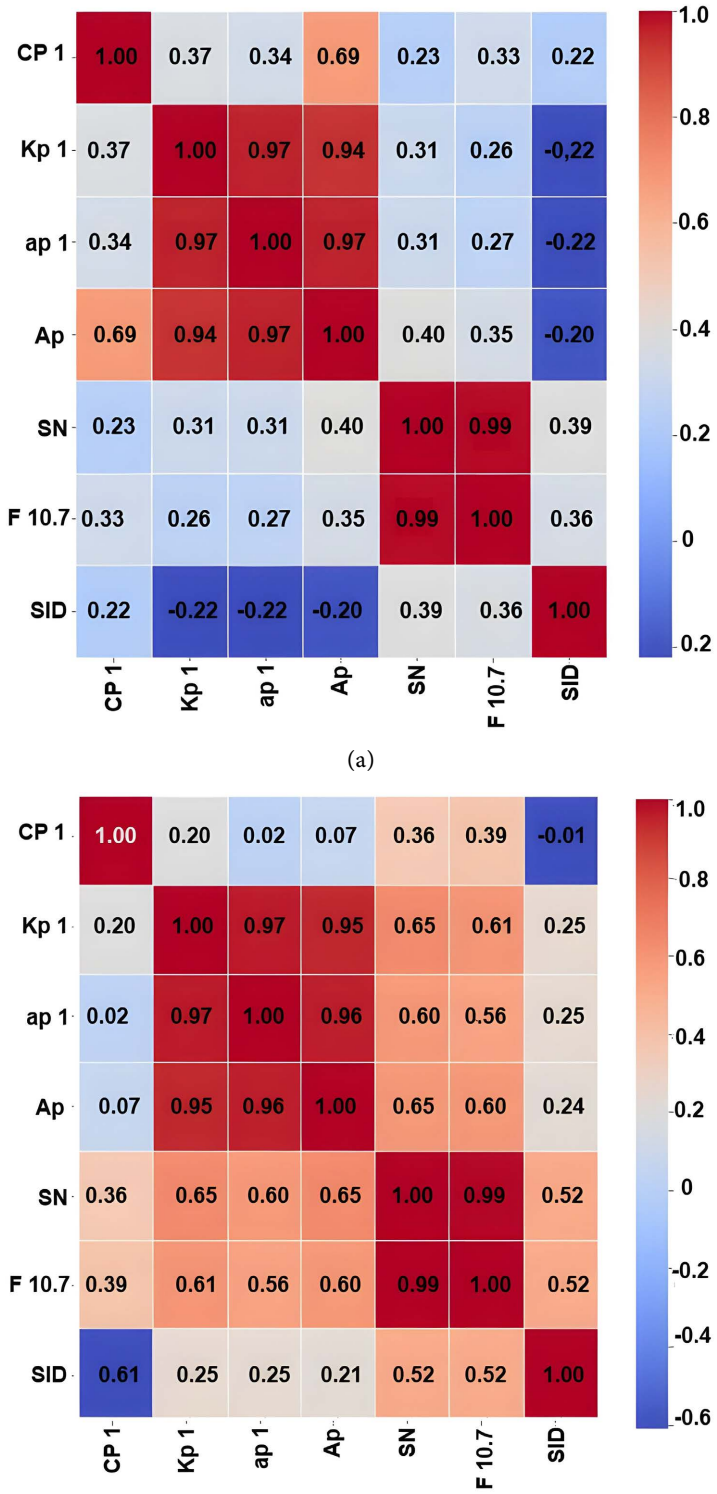

Figure 11. Correlation matrix between AMI Index Scores and Climate Indices for (a) summer and (b) winter.

After identifying the most relevant regions for seasonal variation in AMI deaths during summer and winter, correlations were conducted between these regions

and standardized geomagnetic data, referred to as the Climate Index. Figure 11 presents the correlation matrix between the scores of the first principal component of the AMI indices and the Climate Index for the summer months (a) and the winter months (b).

The correlation matrix highlights that the Ap index is the most significant geomagnetic variable for the AMI Index during the summer months, with a correlation coefficient of 0.69. Conversely, in the winter months, the SID variable emerged as the most relevant, with a correlation coefficient of −0.61. Both correlations are highly significant at the 1% probability level, underscoring the importance of these variables in understanding the seasonal dynamics of AMI mortality.

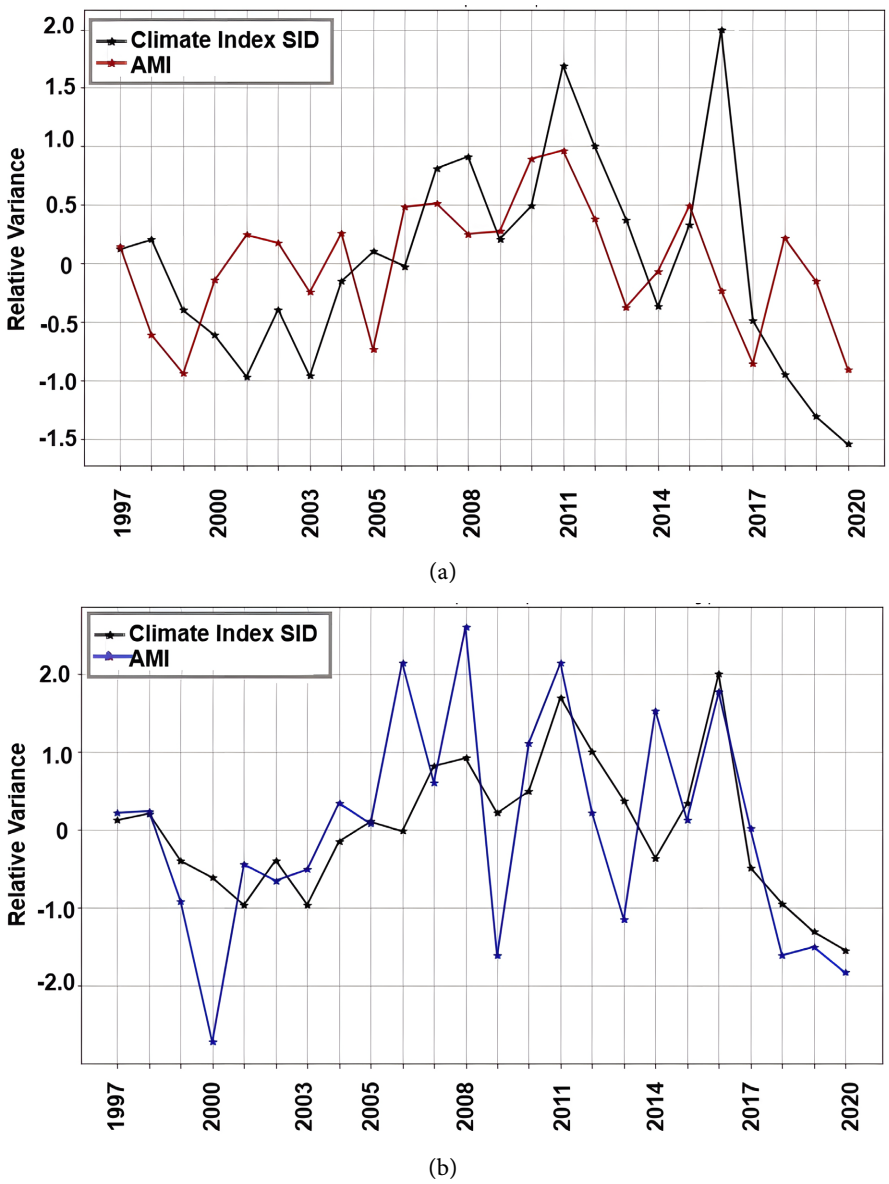

Figure 12. Climate Index SID and AMI deaths that occurred in summer in the states of (a) Rio Grande do Norte and (b) Paraná.

The results of the seasonal analysis reveal notable patterns. During the summer, Bahia (BA) and Sergipe (SE) emerge as particularly influential states, as shown in Figure 12. During this period, the geomagnetic variable Ap is identified as the most relevant in explaining variations among climate variables. Figure 12 illustrates these relationships, highlighting a striking similarity in the time series variations of the Ap index for BA and SE during the summer months.

Conversely, during the winter months, the analysis highlights a distinct dynamic. Figure 13 depicts the variation of the Climate Index SID in Rio Grande do Norte (RN) and Paraná (PR). This suggests that, in winter, these states play a prominent role in climate variations, demonstrating their influence on the relationship between solar activity and AMI mortality.

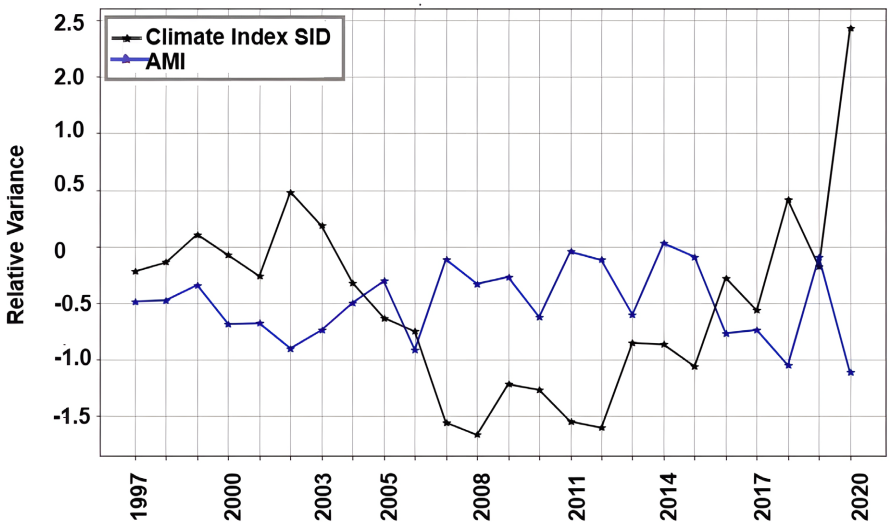

(a)

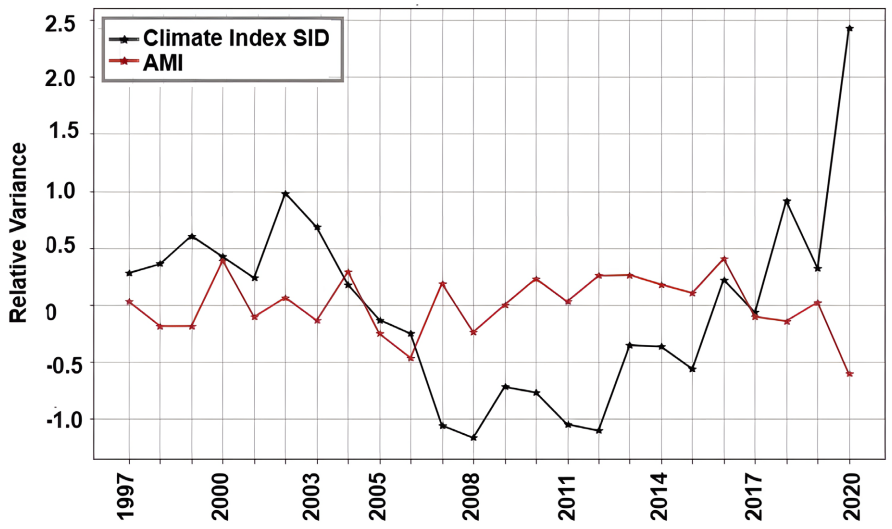

(b)

Figure 13. Climate Index SID and AMI deaths that occurred in winter for (a) Rio Grande do Norte and (b) Paraná.

The dipole observed between the Climate Index Ap in BA and SE during the summer months, and the Climate Index SID in RN and PR during the winter months, is compared with the AMI Death Index. Their extremes are summarized in Table 2, providing a detailed view of these seasonal dynamics.

In Table 2, it becomes evident how extremes in climate indices are associated with peaks in the AMI Death Index in the corresponding regions. This association is particularly pronounced during the summer months, where Bahia (BA) and Sergipe (SE) exhibit positive extremes in the Climate Index Ap, which correlate with significant increases in the AMI Death Index. Similarly, during the winter months, Rio Grande do Norte (RN) and Paraná (PR) show negative extremes in the Climate Index SID, also correlated with increased AMI deaths in these regions.

Table 2. Years with the highest and lowest occurrences of deaths during the winter and summer seasons in states exhibiting a dipole pattern. The abbreviations are as follows: BA (Bahia), SE (Sergipe), RN (Rio Grande do Norte), and PR (Paraná). "Max" refers to the years with the highest AMI (Acute Myocardial Infarction) death rates, while "Min" indicates the years with the lowest death rates.

State	Summer Max (Climate Index)	Winter Max (AMI Index)	Summer Min (Climate Index)	Winter Min (AMI Index)
BA	2016, 2011	2010, 2011	2001, 2003, 2020	1999, 2017, 2020
SE	2011, 2016	2011, 2016	2001, 2003, 2020	2000, 2020
RN	1999, 2018, 2020	2011, 2014	2008, 2012	2018, 2020
PR	2000, 2018, 2020	2000, 2004, 2016	2008, 2012	2006, 2020

These findings suggest that variations in geomagnetic and climatic indices may play a significant role in the occurrence of AMI deaths across different regions of Brazil, with distinct seasonal patterns. Although some evidence supports the relationship between geomagnetic activity and physiological processes, such as heart rate variability (HRV), this connection remains a topic of debate. For instance, [17] and [21] reported inconsistent findings, whereas [22] observed weak correlations between HRV and geomagnetic indices after accounting for autocorrelations in time-series data.

The precise mechanisms through which geomagnetic variations influence biological processes remain unclear, warranting further research, particularly in low-latitude regions. It is also important to acknowledge the limitations inherent to ecological studies. While statistical significance is observed, it does not necessarily imply biological relevance. Confounding factors, which are difficult to control in this type of study, may bias the results and should be carefully considered in future analyses.

Moreover, psychological or biological variables that could explain individual differences in the measured outcomes were not assessed. The analysis also accounted for the unique conditions of the Brazilian population during the study period, including distinctive demographic characteristics, healthcare quality and accessibility, and other factors influencing health outcomes [40]. Consequently,

similar geophysical events may produce varying effects in different populations, underscoring the need for careful interpretation of these findings.

Despite these limitations, this study contributes valuable insights into the potential effects of geomagnetic activity on health, warranting further investigation to elucidate these relationships and their underlying mechanisms, particularly in underexplored regions like Brazil.

4. Conclusions

This study reveals a significant relationship between solar activity and cardiovascular disease mortality rates across different regions of Brazil, with Acute Myocardial Infarction (AMI) identified as the leading cause of death. Regions such as Pernambuco (PE), Rio Grande do Sul (RS), and Paraná (PR) exhibited the highest average AMI mortality rates, with values of 60.4, 56.8, and 58.3 deaths per 100,000 inhabitants, respectively. Temporal trends showed a consistent increase in AMI mortality across most states, except for Santa Catarina (SC), which displayed a different trajectory. These findings highlight the importance of understanding the interplay between solar activity and broader environmental and socioeconomic factors in shaping health outcomes.

Principal Component Analysis (PCA) revealed distinct seasonal patterns, emphasizing the influence of geomagnetic and climatic variables on mortality rates throughout the year. The Ap geomagnetic index showed a strong correlation with AMI mortality during summer, while the SID index had a greater impact during winter. Additionally, a dipole phenomenon was observed, with geomagnetic variations affecting the Northeast (NE) and Southern (S) regions in opposite directions depending on the season. These spatial and temporal variations suggest complex interactions that warrant further investigation to elucidate the underlying mechanisms.

The study significantly contributes to forecasting in biometeorology and public health interventions by exploring the potential effects of geomagnetic activity on biological systems, particularly in relation to cardiovascular health. The findings demonstrate notable associations between geomagnetic indices and mortality rates; however, the mechanisms driving these associations remain poorly understood. Future research should focus on exploring how geomagnetic disturbances interact with cardiovascular, neurological, and immune system functions. Moreover, it is essential to address confounding factors, including air pollution, socioeconomic conditions, and healthcare accessibility, which may influence the observed relationships.

The practical implications of this research are considerable. Public health systems could implement early warning systems to alert populations during periods of heightened geomagnetic activity, enabling healthcare providers and individuals to take preventive measures. Preventive care strategies could be tailored to account for seasonal variations in geomagnetic activity, with a particular focus on vulnerable groups, such as individuals at higher risk of cardiovascular diseases.

Additionally, training programs for healthcare professionals could enhance awareness of the potential health impacts of solar and geomagnetic activity, improving patient care and outcomes.

Despite its contributions, this study is not without limitations. The ecological design restricts the ability to control for individual-level confounding factors, and while statistically significant associations have been identified, these do not always reflect biological relevance. Furthermore, the study emphasizes the need for further research in underexplored regions like Brazil, particularly in low-latitude areas, to validate these findings. Incorporating advanced methodologies, such as machine learning and long-term multivariate analyses, could provide deeper insights into the complex interactions between geomagnetic activity, environmental factors, and health outcomes.

In conclusion, this study enhances the understanding of the intricate relationship between solar activity and cardiovascular mortality. By addressing biological, environmental, and socioeconomic factors in future research, it will be possible to improve the prediction and mitigation of public health risks during periods of heightened solar activity, especially in regions more vulnerable to cardiovascular mortality. The integration of advanced methodologies and a focus on region-specific analyses could further refine the understanding of these associations and guide the development of effective public health interventions.

Acknowledgements

This work was supported by the National Institute of Science and Technology for Climate Change Phase 2 under CNPq Grant 465501/2014-1, FAPESP Grant 2014/50848-9 and the National Coordination for High Level Education and Training (CAPES) Grant 88881.146050/2017-01.

Conflicts of Interest

The authors declare no conflicts of interest regarding the publication of this paper.

References

[1] Wertheimer, N. and Leeper, E. (1979) Electrical Wiring Configurations and Childhood Cancer. *American Journal of Epidemiology*, **109**, 273-284. https://doi.org/10.1093/oxfordjournals.aje.a112681

[2] Marcilio, I., Habermann, M. and Gouveia, N. (2009) Campos magnéticos de frequência extremamente baixa e efeitos na saúde: Revisão da literatura. *Revista Brasileira de Epidemiologia*, **12**, 105-123. https://doi.org/10.1590/s1415-790x2009000200002

[3] Mercola, J. (2020) EMF*D: 5G, Wi-Fi & Cell Phones: Hidden Harms and How to Protect Yourself. Hay House, Inc.

[4] Stoupel, E. (2020) Cosmic Ray and Human Health. *EC Pharmacology and Toxicology*, **8**, 167-176.

[5] Palmer, S.J., Rycroft, M.J. and Cermack, M. (2006) Solar and Geomagnetic Activity, Extremely Low Frequency Magnetic and Electric Fields and Human Health at the Earth's Surface. *Surveys in Geophysics*, **27**, 557-595.

https://doi.org/10.1007/s10712-006-9010-7

[6] Ziubryte, G., Jarusevicius, G., Landauskas, M., Ragulskis, M., McCraty, R. and Vainoras, A. (2021) Cardiovascular System Interactions with the Local Earth Magnetic Field Fluctuations: A Cohort Study. https://doi.org/10.21203/rs.3.rs-250922/v1

[7] Chai, Z., Wang, Y., Li, Y., Zhao, Z. and Chen, M. (2023) Correlations between Geomagnetic Field and Global Occurrence of Cardiovascular Diseases: Evidence from 204 Territories in Different Latitude. *BMC Public Health*, **23**, Article No. 1771. https://doi.org/10.1186/s12889-023-16698-1

[8] Qu, J. and Wickramasinghe, N.C. (2020) The World Should Establish an Early Warning System for New Viral Infectious Diseases by Space-Weather Monitoring. *MedComm*, **1**, 423-426. https://doi.org/10.1002/mco2.20

[9] Alabdulgader, A., McCraty, R., Atkinson, M., Dobyns, Y., Vainoras, A., Ragulskis, M., *et al.* (2018) Long-Term Study of Heart Rate Variability Responses to Changes in the Solar and Geomagnetic Environment. *Scientific Reports*, **8**, Article No. 2663. https://doi.org/10.1038/s41598-018-20932-x

[10] Elhalel, G., Price, C., Fixler, D. and Shainberg, A. (2019) Cardioprotection from Stress Conditions by Weak Magnetic Fields in the Schumann Resonance Band. *Scientific Reports*, **9**, Article No. 1645. https://doi.org/10.1038/s41598-018-36341-z

[11] Geronikolou, S., Leontitsis, A., Petropoulos, V., Davos, C., Cokkinos, D. and Chrousos, G. (2020) Cyclic Stroke Mortality Variations Follow Sunspot Patterns. *F1000Research*, **9**, Article 1088. https://doi.org/10.12688/f1000research.24794.2

[12] McCraty, R., Atkinson, M., Tomasino, D. and Tiller, W.A. (2018) The Electricity of Touch: Detection and Measurement of Cardiac Energy Exchange between People. In: *Brain and Values*, Psychology Press, 359-379. https://doi.org/10.4324/9780203763834-16

[13] Stojan, G., Giammarino, F. and Petri, M. (2021) Systemic Lupus Erythematosus and Geomagnetic Disturbances: A Time Series Analysis. *Environmental Health*, **20**, Article No. 28. https://doi.org/10.1186/s12940-021-00692-4

[14] Ivanovic-Zuvic, F., de La Vega, R., Ivanovic-Zuvic, N. and Correa, E. (2010) Enfermedades afectivas y actividad solar: Seguimiento a 16 años. *Revista médica de Chile*, **138**, 694-700. https://doi.org/10.4067/s0034-98872010000600005

[15] Díaz-Sandoval, R., Erdélyi, R. and Maheswaran, R. (2011) Could Periodic Patterns in Human Mortality Be Sensitive to Solar Activity? *Annales Geophysicae*, **29**, 1113-1120. https://doi.org/10.5194/angeo-29-1113-2011

[16] Mavromichalaki, H., Papailiou, M., Gerontidou, M., Dimitrova, S. and Kudela, K. (2021) Human Physiological Parameters Related to Solar and Geomagnetic Disturbances: Data from Different Geographic Regions. *Atmosphere*, **12**, Article 1613. https://doi.org/10.3390/atmos12121613

[17] Watanabe, Y., Cornélissen, G., Halberg, F., Otsuka, K. and Ohkawa, S.-I. (2000) Associations by Signatures and Coherences between the Human Circulation and Helio and Geomagnetic Activity. *Biomedicine & Pharmacotherapy*, **55**, s76-s83. https://doi.org/10.1016/s0753-3322(01)90008-3

[18] Zilli Vieira, C.L., Alvares, D., Blomberg, A., Schwartz, J., Coull, B., Huang, S., *et al.* (2019) Geomagnetic Disturbances Driven by Solar Activity Enhance Total and Cardiovascular Mortality Risk in 263 U.S. Cities. *Environmental Health*, **18**, Article No. 83. https://doi.org/10.1186/s12940-019-0516-0

[19] Stoupel, E., Kalediene, R., Petrauskiene, J., Starkuviene, S., Abramson, E., Israelevich, P. and Sulkes, J. (2007) Monthly Deaths Number and Concomitant Environmental

Physical Activity: 192 Months Observation (1990-2005). *Sun Geosph*, **2**, 78-83.

[20] Mendoza, B. and Sánchez de la Peña, S. (2010) Solar Activity and Human Health at Middle and Low Geomagnetic Latitudes in Central America. *Advances in Space Research*, **46**, 449-459. https://doi.org/10.1016/j.asr.2009.06.021

[21] Dimitrova, S., Angelov, I. and Petrova, E. (2013) Solar and Geomagnetic Activity Effects on Heart Rate Variability. *Natural Hazards*, **69**, 25-37. https://doi.org/10.1007/s11069-013-0686-y

[22] Mattoni, M., Ahn, S., Fröhlich, C. and Fröhlich, F. (2020) Exploring the Relationship between Geomagnetic Activity and Human Heart Rate Variability. *European Journal of Applied Physiology*, **120**, 1371-1381. https://doi.org/10.1007/s00421-020-04369-7

[23] IBGE (2010) Conheça cidades e estados do Brasil, Rio de Janeiro: IBGE. https://cidades.ibge.gov.br/

[24] Peel, M.C., Finlayson, B.L. and McMahon, T.A. (2007) Updated World Map of the Köppen-Geiger Climate Classification. *Hydrology and Earth System Sciences*, **11**, 1633-1644. https://doi.org/10.5194/hess-11-1633-2007

[25] Echer, E., Lucas, A.D., Hajra, R., Franco, A.M.D.S., Bolzan, M.J.A. and Nascimento, L.E.S.D. (2023) Geomagnetic Activity Following Interplanetary Shocks in Solar Cycles 23 and 24. *Brazilian Journal of Physics*, **53**, Article No. 79. https://doi.org/10.1007/s13538-023-01294-w

[26] Brazilian Institute of Geography and Statistics (IBGE) (2020) Censo Demográfico 2020: Resultados Preliminares. https://www.ibge.gov.br

[27] Hathaway, D.H. (2010) The Solar Cycle. *Living Reviews in Solar Physics*, **7**, Article No. 1. https://doi.org/10.1007/lrsp-2010-1

[28] Tapping, K.F. (2013) The 10.7 Cm Solar Radio Flux (f10.7). *Space Weather*, **11**, 394-406. https://doi.org/10.1002/swe.20064

[29] Gopalswamy, N., Xie, H., Akiyama, S., Mäkelä, P., Yashiro, S. and Michalek, G. (2015) The Peculiar Behavior of Halo Coronal Mass Ejections in Solar Cycle 24. *The Astrophysical Journal*, **804**, L23. https://doi.org/10.1088/2041-8205/804/1/l23

[30] Royal Observatory of Belgium (2022) SILSO Data/Image, Brussels. https://www.sidc.be/silso/datafiles

[31] Balogh, A., Hudson, H.S., Petrovay, K. and von Steiger, R. (2014) Introduction to the Solar Activity Cycle: Overview of Causes and Consequences. *Space Science Reviews*, **186**, 1-15. https://doi.org/10.1007/s11214-014-0125-8

[32] Pesnell, W.D. (2016) Predictions of Solar Cycle 24: How Are We Doing? *Space Weather*, **14**, 10-21. https://doi.org/10.1002/2015sw001304

[33] Clilverd, M.A., Rodger, C.J., Dietrich, S., Raita, T., Ulich, T., Clarke, E., *et al.* (2010) High-Latitude Geomagnetically Induced Current Events Observed on Very Low Frequency Radio Wave Receiver Systems. *Radio Science*, **45**, 1-11 https://doi.org/10.1029/2009rs004215

[34] Davies, K. (1990) Ionospheric Radio. Peter Peregrinus Ltd.

[35] Romeo, S., Zeni, O., Sannino, A., Lagorio, S., Biffoni, M. and Scarfì, M.R. (2021) Genotoxicity of Radiofrequency Electromagnetic Fields: Protocol for a Systematic Review of *in Vitro* Studies. *Environment International*, **148**, Article 106386. https://doi.org/10.1016/j.envint.2021.106386

[36] Liu, L., Wan, W., Chen, Y. and Le, H. (2011) Solar Activity Effects of the Ionosphere: A Brief Review. *Chinese Science Bulletin*, **56**, 1202-1211. https://doi.org/10.1007/s11434-010-4226-9

[37] Bodewein, L., Schmiedchen, K., Dechent, D., Stunder, D., Graefrath, D., Winter, L., *et al.* (2019) Systematic Review on the Biological Effects of Electric, Magnetic and Electromagnetic Fields in the Intermediate Frequency Range (300 Hz to 1 MHz). *Environmental Research*, **171**, 247-259. https://doi.org/10.1016/j.envres.2019.01.015

[38] Clette, F., Cliver, E.W., Lefèvre, L., Svalgaard, L. and Vaquero, J.M. (2015) Revision of the Sunspot Number(s). *Space Weather*, **13**, 529-530. https://doi.org/10.1002/2015sw001264

[39] Valdés Abreu, J.C. (2023) Degradation of the Global Navigation Satellite System Positioning Accuracy Caused by Ionospheric Disturbance Sources. Universidad de Chile. https://repositorio.uchile.cl/handle/2250/193060

[40] Pandit, D., Ghimire, B., Amory-Mazaudier, C., Fleury, R., Chapagain, N.P. and Adhikari, B. (2021) Climatology of Ionosphere over Nepal Based on GPS Total Electron Content Data from 2008 to 2018. *Annales Geophysicae*, **39**, 743-758. https://doi.org/10.5194/angeo-39-743-2021

[41] Matzka, J., Stolle, C., Yamazaki, Y., Bronkalla, O. and Morschhauser, A. (2021) The Geomagnetic *Kp* Index and Derived Indices of Geomagnetic Activity. *Space Weather*, **19**, e2020SW002641. https://doi.org/10.1029/2020sw002641